

## COMPOSITIONAL AND MICROSTRUCTURAL EVOLUTION OF OLIVINE UNDER MULTIPLE-CYCLE PULSED LASER IRRADIATION AS REVEALED BY FIB/FIELD-EMISSION TEM.

R. Christoffersen<sup>1</sup>, M. J. Loeffler<sup>2</sup>, C. A. Dukes<sup>3</sup>, L.P. Keller<sup>4</sup> and R. A. Baragiola<sup>3,†</sup>, <sup>1</sup>Jacobs, NASA Johnson Space Center, Mail Code XI3, Houston, TX 77058, USA ([roy.christoffersen-1@nasa.gov](mailto:roy.christoffersen-1@nasa.gov)), <sup>2</sup>NASA GSFC, Greenbelt, MD 20771, USA, <sup>3</sup>University of Virginia, Laboratory of Atomic and Surface Physics, Charlottesville, VA 22904, USA, <sup>4</sup>NASA Johnson Space Center, Mail Code XI3, Houston, TX 77058, USA, <sup>†</sup>deceased.

**Introduction:** The use of pulsed laser irradiation to simulate the short duration, high-energy conditions characteristic of micrometeorite impacts is now an established approach in experimental space weathering studies [1, 2]. The laser generates both melt and vapor deposits that contain nanophase metallic Fe (npFe<sup>0</sup>) grains with size distributions and optical properties similar to those in natural impact-generated melt and vapor deposits [3]. There remains uncertainty, however, about how well lasers simulate the mechanical work and internal (thermal) energy partitioning that occurs in actual impacts [4]. We are currently engaged in making a direct comparison between the products of laser irradiation and experimental/natural hypervelocity impacts. An initial step reported here is to use analytical SEM and TEM to attain a better understanding of how the microstructure and composition of laser deposits evolve over multiple cycles of pulsed laser irradiation.

**Experimental Methods:** We irradiated pressed-powder pellets and a single crystal of San Carlos olivine (Fo<sub>90</sub>) with sequential rastered pulses of a GAM ArF excimer laser [5]. SEM and TEM results are reported here for pressed-powder (PP) pellets irradiated with a single rastered scan (1-scan PP) and 99 rastered scans (99-scan PP), and a single crystal (SC) irradiated with 6 scans (6-scan SC). The surfaces of the samples were characterized by SEM imaging after irradiation and areas were selected for FIB cross sectioning for TEM study using an FEI Quanta dual-beam electron/focused ion beam instrument. FIB sections were characterized using a JEOL2500SE analytical field-emission scanning transmission electron microscope (FE-STEM) optimized for quantitative element mapping at <10 nm spatial resolutions.

**Results:** In the SEM, the 99-scan PP sample shows a complex, inhomogeneous, distribution of laser-generated material, largely concentrated in narrow gaps and larger depressions between grains. Local concentrations of npFe<sup>0</sup> spherules 0.1 to 1 μm in size occur within these deposits in SEM back-scatter images. Fig. 1 shows bright-field STEM (BF-STEM) images of a FIB cross-section of a one of these deposits that continuously covers the top and sloping side of an olivine grain. The deposit has 3 microstructurally distinct sub-layers composed of silicate glass with varying modal fractions and size distributions of npFe<sup>0</sup> spherules,

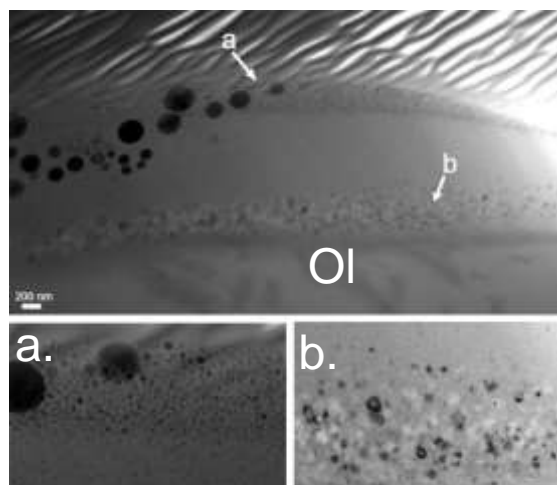


*Fig. 1. Top: Bright-field FE-STEM image of layers of laser-deposited material on Fo<sub>90</sub> olivine grain (Ol) in 99-pulse pressed pellet sample. (a) Detailed microstructure of surface layer containing nanophase metallic Fe spherules, (b) Detailed microstructure of nanocrystalline olivine layer in glassy matrix adjacent to underlying host olivine.*

along with nanocrystalline silicate material (Fig. 1). A relatively thin (50-300 nm) topmost surface layer has a high-concentration of npFe<sup>0</sup> spherules 5-20 nm in size (Fig. 1a). Element mapping shows the layer to be enriched in Fe by a factor of 2.5 relative to the olivine substrate, with Mg and Si depleted by 20% and 10% respectively. This is compositionally complementary to the underlying, middle layer of the deposit that is depleted in Fe, enriched in Mg and has a much lower npFe<sup>0</sup> concentration. A third layer of nanocrystalline olivine occurs at the substrate interface.

On the FE-STEM scale, the layers of laser-generated material on the 1-scan PP and 6-scan SC samples are microstructurally and compositionally less complex than the 99-scan PP sample. The layers continuously cover their respective olivine grains and have uniform widths (125-150 μm) across their respective FIB sections. The layer on the 1-scan PP sample is slightly wider on average (~150 μm) than on the 6-scan SC (~125 μm, Fig. 2). Conventional bright-field and Z-contrast STEM imaging shows the layers in both samples to be similarly composed of <10 npFe<sup>0</sup> spherules in a silicate glass matrix (Figs. 2, 3). The layers in both samples exhibit a distinctive “nanostratigraphy” in their

modal npFe<sup>0</sup> concentrations and grain size (Figs. 2, 3). This npFe<sup>0</sup> microstructural nanostratigraphy is not mirrored in strong variations in major element concentrations determined from compositional profiles extracted from X-ray EDX spectrum images (Fig. 3). The bulk compositions integrated over the layer volumes do, however, differ from the underlying olivine in showing significant Si-depletion relative to Mg+Fe. FE-STEM electron energy loss (EELS) spectroscopy analyses are currently ongoing to correlate both bulk and nanoscale variations in Fe oxidation state within the layers.

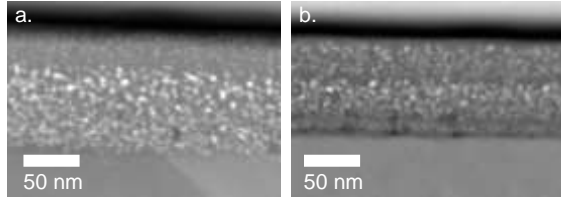


Fig. 2. High-angle annular dark field (HAADF) Z-contrast STEM images of laser-generated layers on olivine grain in 1-scan PP (a) and 6-scan SC (b) samples.

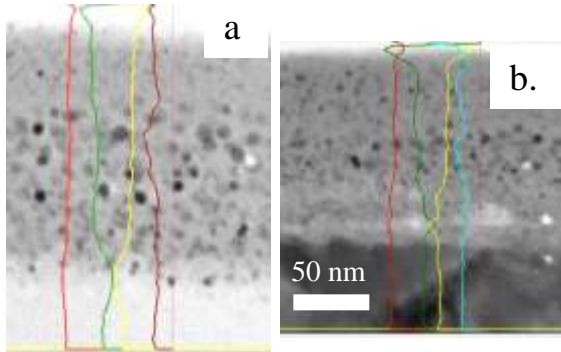


Fig. 3. Wt. % element compositional profiles for elements O, Mg, Si and Fe (left to right) overlain on same-scale BF-STEM images of laser-deposited layer in 1-scan PP (a) and 6-scan SC olivine samples (b). Profiles extracted from X-ray EDX compositional spectrum images.

**Discussion:** We interpret the nanoscale microstructural and compositional variations in the 1-scan PP and 6-pulse SC samples to reflect very short time scale sequential deposition and mixing of melt and vapor-generated material as the pulsed laser beam tracks over the sample. The vapor component in particular, along with small scale thermal variations, likely account for the nanostratigraphic variations in npFe<sup>0</sup> concentration and grain size. For the 99-scan PP, the more complex microstructural/compositional layering reflects longer timescale deposition on an irregular surface that causes build up of thicker, more inhomogeneous and complex deposits. FE-STEM results suggest the topmost layer in the 99-scan PP is a vapor deposit, underlain by a thick-

er microstructurally complex melt-generated layer. The compositional relations suggest the melt layer was partially vaporized, preferentially losing more volatile elements (e.g., Fe). The vaporized material recondensed to form the thin, npFe<sup>0</sup>-rich surface deposit during or immediately after the scan cycle. Nanocrystalline olivine that grew within the melt layer as it formed and cooled is similar in volume and microstructure to what we have observed in the impact melt lining of a micrometeorite impact crater in olivine [6, 7]. This suggests the time-temperature relations attained in the laser sample may not be too different from a micrometeorite impact. Our TEM observations, however, do not show evidence for the same level of mechanical damage (e.g., fracturing) seen around the natural micrometeorite crater [6, 7].

**References:** [1] Moroz L.V. et al. (2014) *Icarus* 235, 187. [2] Sasaki S. et al. (2001) *Nature* 410, 555. [3] Brunetto R. et al. (2007) *Icarus* 191, 381. [4] Gault, D. E. and E. D. Heitowitz (1963) Proc. Hy. V. Impact Sym, NASA, 25. [5] Loeffler M. J. et al. (2016) *MAPS*, in press. [6] Noble, S.K. et al. (2015) S. W. Airless Bodies Workshop, LPI, #1465. [7] Noble S. K. et al. (2016) 47<sup>th</sup> LPSC, submitted.